

Received July 31, 2018, accepted September 24, 2018, date of publication October 15, 2018, date of current version November 9, 2018.

Digital Object Identifier 10.1109/ACCESS.2018.2875925

Array Gain Analysis in Molecular MIMO Communications

MARTIN DAMRATH¹, (Student Member, IEEE),
H. BIRKAN YILMAZ², (Member, IEEE),
CHAN-BYOUNG CHAE², (Senior Member, IEEE),
AND PETER ADAM HOEHER¹, (Fellow, IEEE)

¹Faculty of Engineering, University of Kiel, 24143 Kiel, Germany

²School of Integrated Technology, Yonsei Institute of Convergence Technology, Yonsei University, Incheon 406-840, South Korea

Corresponding author: Martin Damrath (md@tf.uni-kiel.de)

The work of H. B. Yilmaz and C.-B. Chae was supported in part by the Basic Science Research Program through the NRF of Korea under Grant 2017R1A1A1A05001439 and Grant 2016K2A9A1A06926542 and in part by the Ministry of Science and ICT, South Korea, through the ICT Consilience Creative Program under Grant IITP-2018-2017-0- 01015.

ABSTRACT In this paper, spatial transmission techniques in the area of multiple-input multiple-output (MIMO) diffusion-based molecular communications (DBMC) are investigated. For transmitter-side spatial coding, Alamouti-type coding and repetition MIMO coding are analyzed. At the receiver-side, selection diversity and equal-gain combining are studied as combining strategies. Throughout the numerical analysis, a symmetrical 2×2 MIMO-DBMC system is assumed. Furthermore, a trained artificial neural network is utilized to acquire the channel impulse responses. The numerical analysis demonstrates that there is no spatial diversity gain in the DBMC system under investigation, but that it is possible to achieve an array gain instead. In addition, it is shown that for MIMO-DBMC systems repetition MIMO coding is superior to Alamouti-type coding.

INDEX TERMS Array gain, artificial neural network, channel modeling, molecular communication via diffusion, multiple-input multiple-output, spatial diversity.

I. INTRODUCTION

Molecular communication (MC), a biologically inspired communication paradigm, utilizes molecules as information carriers [1], [2]. MC is claimed to be a key technology in realizing autonomous nanomachines (NMs) [3], the size of which ranges from several nanometers up to a few micrometers [4]. Due to their size, NMs are restricted with respect to their energy budget and capabilities [5], [6], while MC provides an energy-efficient biocompatible method of communication. Consequently, the capability of NMs can be enhanced by working as a swarm [2], [7]. MC can be used in the industrial and consumer sectors, such as with food and water quality control or intelligent textile fabrics. MC can also be utilized in the environmental field, such as with biodegradation or air pollution control. The main application, however, is anticipated to be in the medical sector, where NMs can be used for applications like targeted drug delivery, tissue engineering, or health monitoring [3], [6]. Nevertheless, MC can also be used in macro-scale applications, especially in

environments where radio-based communication do not work well, such as pipes or mines.

Diffusion-based molecular communication (DBMC) [8] is a passive form of MC. Following the law of diffusion, messenger molecules propagate passively from a source to a sink. This offers an energy efficient way of communication, because the energy for propagation comes directly from the environment. However, the communication channel is fundamentally different from the classical radio-based wireless communication channel. In fact, radio waves propagate deterministically in a given environment, whereas molecules perform a random walk. As a result, the diffusive propagation channel possess a slowly decreasing stochastic channel impulse response. Consequently, DBMC systems suffer from intersymbol interference (ISI) and unreliable transmission [9]. In multiple-input multiple-output (MIMO) scenarios, link reliability can be improved by exploiting multiple transmit and/or receive antennas.

In classical wireless communications, MIMO techniques already appertain to the state-of-the-art. In molecular communication, however, they have just rarely been considered. To the best of our knowledge, the first conjunction between MC and MIMO was given in [10]. The authors introduced transmitter diversity, receiver-side diversity combining, and spatial multiplexing to the area of DBMC. While focusing on multi-user interference, the effect of ISI was paid little attention throughout the work. In [11], several detection algorithms are proposed for spatial multiplexing scenarios in DBMC and it is shown, by a proof of concept testbed implementation, that utilizing a molecular MIMO concept has potential to increase the data rate. In contrast to [10], Koo *et al.* [11] took both, ISI and interlink interference (ILI), in their channel model into account. Furthermore, they extended their tabletop molecular single-input single-output (SISO) testbed to a MIMO testbed. Lu *et al.* [12] expanded a MC broadcast system by a second absorbing receiver and studied the effect on the bit error ratio (BER) and the channel capacity. However, authors considered asymptotic behavior (i.e., $t \rightarrow \infty$) without solving the time dependent capture probabilities, which is an open problem in the literature. Therefore, we utilize artificial neural network (ANN) to model the MIMO channel with multiple absorber receiver apertures. Murin *et al.* [13] interpreted each individual transmission paths of an information particle as a single-input multiple-output (SIMO) channel. With focus on one-shot communication over a molecular timing channel, they studied the system diversity gain depending on the number of released particles.

The focus of this paper is on a DBMC MIMO channel taking ISI as well as ILI into account. The main contribution is a study of different spatial algorithms at the transmitter and at the receiver sides. At the transmitter side, we propose and analyze two different spatial coding techniques, namely Alamouti-type coding and repetition MIMO coding. At the receiver side, we focus on two different receiver combining strategies: Selection diversity and equal-gain combining. The latter strategy is the same as maximum-ratio combining in symmetrical scenarios. In terms of BER simulations, we analyze the influence of key system parameters on the system performance and perform comparison to a SISO scenario. Furthermore, we show that there is no spatial diversity, but an array gain that can be achieved in the DBMC channel under investigation. Within the numerical simulations, we used a trained ANN to acquire the MIMO channel impulse responses.

The remainder of this paper is organized as follows: Section II summarizes a 2×2 MIMO system model that is assumed throughout this work. Section III presents how MIMO channel impulse responses are acquired by a trained ANN. Section IV proposes, based on the system model, spatial coding techniques, as well as receiver combining strategies for molecular MIMO systems. Section V presents the detection algorithms that are applied in the numerical analysis in Section VI. When necessary, the detection algorithms are

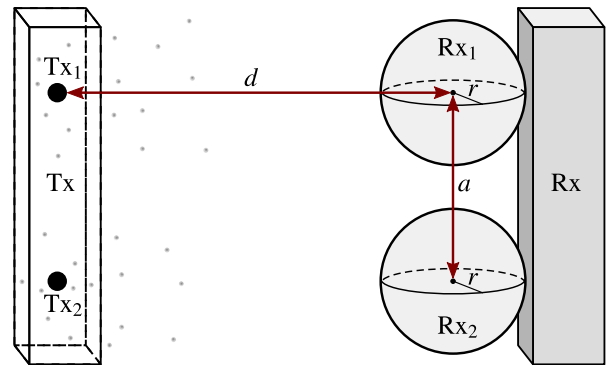


FIGURE 1. Model of the diffusion-based molecular 2×2 MIMO system under investigation [11].

adapted to the 2×2 MIMO scenario. Finally, Section VII summarizes the work and gives an outlook for future work.

II. SYSTEM MODEL

A. TOPOLOGY AND PROPAGATION MODEL

The system model under investigation, shown in Fig. 1, is similar to the system model introduced in [11] and [14]. It contains a static transmitter Tx and a static receiver Rx within a fluid medium. The Rx has two spherical receive apertures Rx1 and Rx2 with radius r attached to its reflecting body. The Tx consists of two point-emitters Tx1 and Tx2. Subsequently, the receive apertures and the emitters are called antennas. Tx1 and Tx2 are directly aligned to Rx1 and Rx2. Consequently, the distance between Tx1 and Rx1, as well as that between Tx2 and Rx2, is given as d . Furthermore, the separation distance between Tx1 and Tx2, as well as between Rx1 and Rx2, is given as a . As a result, Tx and Rx form a symmetrical 2×2 MIMO system. The fluid medium is assumed to be homogeneous, three-dimensional infinitely spatially extended, and has no drift. Accordingly, it is described by the constant diffusion coefficient D .

The molecules emitted by Tx1 and Tx2 propagate by Brownian motion, which is described by the Wiener process [15]. The Wiener process $W(t)$ is characterized as follows:

- $W(0) = 0$,
- $W(t)$ is almost surely continuous,
- $W(t)$ has independent increments,
- $W(t_2) - W(t_1) \sim \mathcal{N}(0, \phi(t_2 - t_1))$ for $0 \leq t_1 \leq t_2$,

where $\mathcal{N}(\mu, \sigma^2)$ is the Gaussian distribution with mean μ and variance σ^2 . The variance of the step length in one dimension is a function of the duration, more specifically it is $\phi(t_2 - t_1) = 2D(t_2 - t_1)$ for Brownian motion. Simulating the Brownian motion includes consecutive steps in an n -dimensional space that obeys to Wiener process dynamics. For an accurate simulation, time is divided into sufficiently small time intervals (Δt) and at each time interval molecules take random steps in each dimension. In an n -dimensional

space, a random step is given as:

$$\begin{aligned} \Delta \mathbf{r} &= (\Delta r_1, \dots, \Delta r_n) \\ \Delta r_i &\sim \mathcal{N}(0, 2D\Delta t) \quad \forall i \in \{1, \dots, n\}, \end{aligned} \quad (1)$$

where Δr and Δr_i correspond to random displacement vector and displacement at the i th dimension.

Rx_1 and Rx_2 are assumed to be perfect absorbing and counting receivers. Accordingly, a diffusing molecule will be counted and removed from the environment the first time it hits to a receiving sphere. As a result, the time histogram of absorbed molecules at Rx_1 and Rx_2 follow the first passage time concept. Assuming just a single absorbing spherical receiver inside a 3-dimensional (3-D) environment, the probability that a molecule hits the receiver until time t after its release is given as [16]:

$$F(t) = \frac{r}{d} \operatorname{erfc}\left(\frac{d-r}{\sqrt{4Dt}}\right), \quad (2)$$

where $\operatorname{erfc}(\cdot)$ denotes the complementary error function. For multiple absorbing spherical receivers, unfortunately, there does not exist an equivalent closed-form expression. Consequently, for a given MIMO scenario (2) has to be obtained by a random-walk-based simulation. Alternatively, it can be acquired by using a trained ANN, as presented in Section III.

B. COMMUNICATION CHANNEL

The modulation scheme under investigation is on-off keying (OOK) [17]–[19]. Tx_i emits either no molecules or N messenger molecules at the beginning of a symbol period of length T_s to represent bit $u_i[k] = 0$ or $u_i[k] = 1$, respectively. Accordingly, molecules emitted by Tx_1 and Tx_2 are of the same type. They are assumed to be the only molecules in the medium; i.e., there is no background noise caused by molecules that are initially present in the medium. Furthermore, Rx is assumed to be synchronized with Tx in time domain. As an example, time synchronization can be achieved by an external signal like the human heart-beat or, as suggested in [20], by releasing inhibitory molecules. In addition, Rx_1 and Rx_2 perform strength/energy detection [21]–[23]. Consequently, the number of hitting molecules at each receive antenna is accumulated for each bit period separately.

The MIMO channel can be represented by a superposition of all subchannels. Here, a subchannel is defined as the channel between the transmit antenna Tx_i and the receive antenna Rx_j . Accordingly, each subchannel can be characterized by the corresponding channel coefficients $h_{ji}[\ell]$ ($0 \leq \ell \leq L$) and can be represented by an equivalent discrete-time channel model with the effective channel memory length L [24], [25]. For infinite channel memory length, L should be chosen at least as large as the transmitted sequence length. Depending on the system parameters, L can be further reduced to the channel coefficients that carry most of the energy without significantly affecting the results.

Superimposing all subchannels related to Rx_j will lead to the total number of received molecules at Rx_j :

$$y_j[k] = \sum_{i=1}^{N_{Tx}} \sum_{\ell=0}^L h_{ji}[\ell] x_i[k-\ell] + n_j[k], \quad (3)$$

where N_{Tx} is the total number of transmitters, $h_{ji}[\ell]$ describes the probability that a molecule hits Rx_j during the ℓ th time slot after its emission at Tx_i , $x_i[k]$ is the discrete-time representation of the modulated data symbol transmitted by Tx_i at the start of the k th transmission interval, and $n_j[k]$ describes the amplitude dependent noise caused by the diffusive propagation of the molecules. For OOK, which is assumed throughout this paper, $x_i[k]$ is defined as

$$x_i[k] = \begin{cases} N & \text{if } u_i[k] = 1 \\ 0 & \text{if } u_i[k] = 0. \end{cases} \quad (4)$$

The event that a single molecule emitted by Tx_i is absorbed by Rx_j during a certain time period can be modeled by a Bernoulli trial with success probability $h_{ji}[\ell]$. Accordingly, the absorption event of N molecules can be described by a binomial distribution [26]. As a result, the distribution of (3) follows the sum of several binomial distributions:

$$y_j[k] \sim \sum_{i=1}^{N_{Tx}} \sum_{\ell=0}^L \mathcal{B}(x_i[k-\ell], h_{ji}[\ell]), \quad (5)$$

where $\mathcal{B}(M, p)$ describe a binomial distribution with M number of trials and success probability p . This channel model is known as the Poisson-binomial channel model.

Assuming a SISO scenario, the channel coefficients can be easily determined from (2):

$$h[\ell] = F((\ell + 1)T_s) - F(\ell T_s). \quad (6)$$

If there is more than one absorbing sphere present inside the medium, the closed-form analytical solution is not available in the literature and $h_{ji}[\ell]$ have to be determined. One method includes to run random-walk-based simulations, another method is to utilize a trained ANN as presented in Section III.

III. ANN FOR CHANNEL MODELING

For the rest of the work, we need the channel coefficients. If the molecule arrival function has a closed-form solution for the given topology, the channel coefficients are acquired by utilizing the closed-form solution. However, for absorbing receivers, in general closed-form solutions exist only for very simple topologies (e.g., single absorbing spherical receiver with a point source). Hence, Monte Carlo simulations are done in general to obtain the channel coefficients. In this work, we use the trained ANN from our previous work [27] to model a molecular MIMO channel. Note that the trained ANN is used for channel modeling, rather than for channel estimation in our communication system. A trained ANN is able to estimate the mean channel coefficients $h_{ji}[\ell]$ for a given MIMO scenario. Please note that a trained ANN

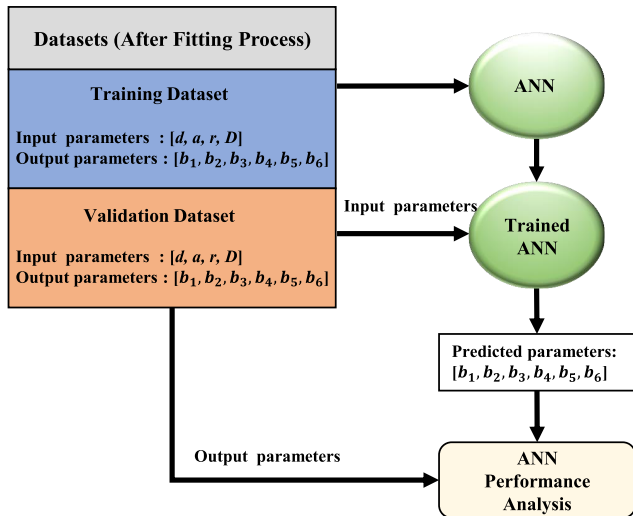


FIGURE 2. The flowchart and the dataset structure of the ANN training process. After curve fitting, the input-output pairs are fed to the training process, where the input is (d, a, r, D) and the output is the model parameters (i.e., b_i 's).

does not require any simulation data while we need simulations for the training phase.

For training the ANN, we use three fully connected layers and we use back-propagation with Bayesian regularization to cope with over-learning, which updates the weights and bias values according to Levenberg-Marquardt optimization. Training data set consists of 150 cases which are obtained by utilizing a modified SISO channel response function for fitting to the data of extensive simulations. Details of the ANN processes can be found in [27]. Please note that, in a 2×2 molecular MIMO scenario, we have two different spherical absorbing receivers – Rx_1 and Rx_2 – so that we need to model, for each receive antenna, two different channel impulse response functions per receive antenna, which depend on the distances.

We consider a case in which only Tx_1 emits molecules for analyzing the cumulative channel impulse response functions at Rx_1 (i.e., $F_{11}(\cdot)$) and at Rx_2 (i.e., $F_{21}(\cdot)$) for modeling the received signal. Due to the rectangular symmetry, formulating $F_{11}(\cdot)$ and $F_{21}(\cdot)$ enables us to obtain $F_{22}(\cdot) = F_{11}(\cdot)$ and $F_{12}(\cdot) = F_{21}(\cdot)$. The modified channel impulse response function at Rx_1 is given as follows:

$$F_{11}(t, b_1, b_2, b_3) = b_1 \frac{r}{d} \operatorname{erfc} \left(\frac{d-r}{(4D)^{b_2} t^{b_3}} \right), \quad (7)$$

where b_1, b_2 , and b_3 represent the model fitting parameters. These model-fitting parameters are introduced so as to compensate for the discrepancy between the SISO and MIMO models. Similarly we define the response at Rx_2 (due to the cross link interference) as follows:

$$F_{21}(t, b_4, b_5, b_6) = b_4 \frac{r}{\sqrt{d^2+a^2}} \operatorname{erfc} \left(\frac{\sqrt{d^2+a^2}-r}{(4D)^{b_5} t^{b_6}} \right), \quad (8)$$

where b_4, b_5 , and b_6 are model fitting parameters.

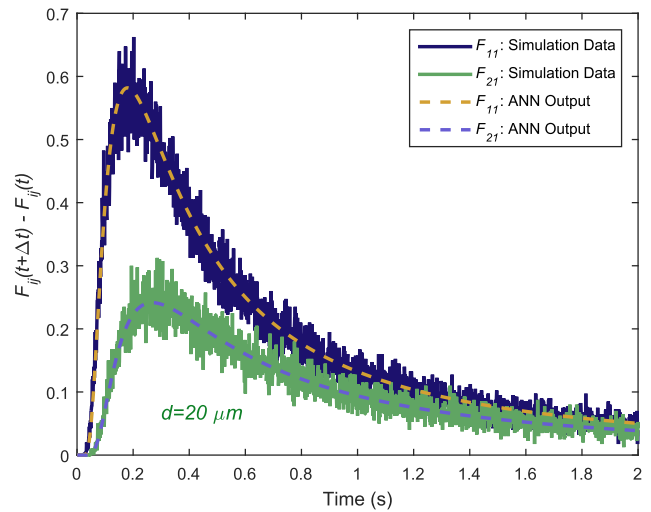


FIGURE 3. ANN and simulation data comparison for channel impulse response functions after Tx_1 emits 3000 molecules ($d=20 \mu\text{m}$, $\sigma=13 \mu\text{m}$, $r=5 \mu\text{m}$, $D=200 \mu\text{m}^2/\text{s}$, $\Delta t=0.001 \text{ s}$).

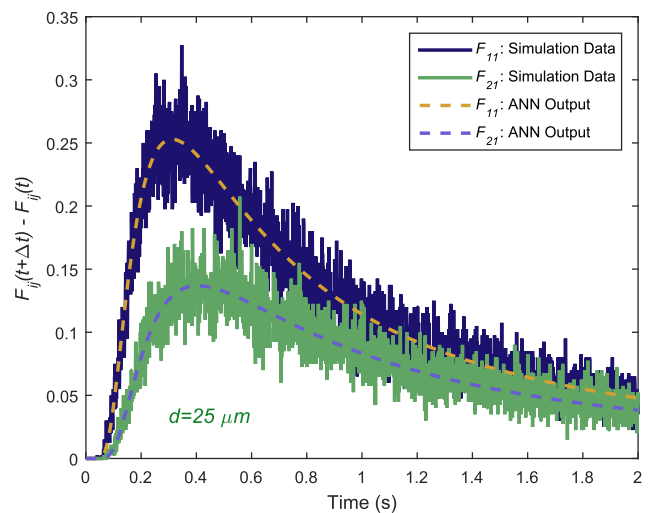


FIGURE 4. ANN and simulation data comparison for channel impulse response functions after Tx_1 emits 3000 molecules ($d=25 \mu\text{m}$, $\sigma=13 \mu\text{m}$, $r=5 \mu\text{m}$, $D=200 \mu\text{m}^2/\text{s}$, $\Delta t=0.001 \text{ s}$).

To find the b_i values, we use a nonlinear least squares curve-fitting technique on the simulation data. These values are the basis of the training and test datasets with the scenario parameters (Fig. 2). Hence, the output of the curve-fitting process consists of the model parameters for each specific scenario. After forming the training and test datasets, the training data is fed into the ANN training process. Note that the trained ANN only requires the system parameters such as d, a, r , and D (no simulation data).

In Figs. 3 and 4, we present the resulting channel impulse functions with a time resolution of 0.001 s for simulation and ANN technique. The received signal at the intended receiver (i.e., F_{11} or F_{22}) and the ILI signal from the simulations are coherent with the ANN results. Therefore, we can utilize

the output of the ANN to obtain channel coefficients for evaluating the number of received molecules and simulating the consecutive data transmissions. Depending on the symbol duration, we can evaluate the channel response for each symbol slot.

In Fig. 5, we present the channel coefficients that are acquired from extensive simulations and the trained ANN. We plot the $h_{11}[k]$ and $h_{21}[k]$ values by utilizing F_{11} , F_{21} , and the symbol duration. The first observation is that the simulation and ANN results match well. Our results validate and support the usage of ANN to obtain the channel coefficients. Second, we observe that without equalization the symbol duration of 0.4 s is not sufficient for $d = 25 \mu\text{m}$. Thus, we clearly see the effect of distance on the channel coefficients while designing an MC system. For a $d = 25 \mu\text{m}$ case (stems with triangle marker), the channel coefficient value at the current symbol slot is smaller than the first ISI symbol slot, which is also supported by Fig. 4 due to the peak time. Therefore, with the help of the trained ANN, we are able to design a suitable symbol duration T_s for the cases of interest.

For the MIMO array gain analysis, we will directly use the outputs of the trained ANN (i.e., the channel coefficients) without any need for simulations. For a wide range of parameters, we observe that the trained ANN performs sufficiently accurate without knowing the simulation data that is used for validation. Hence, the use of a trained ANN eases the process of gain analysis and eliminates the necessity of particle-based simulations.

IV. SPATIAL CODING AND COMBINING TECHNIQUES

In the case of multiple antennas at the transmitter and/or receiver side, it is well-known that a spatial diversity gain can be achieved in wireless radio communication. This gain usually comes from spatial coding along multiple transmit antennas and/or receiver combining strategies given multiple receive antennas. In the sense of spatial coding, the same information is transmitted via several antennas. The information is typically represented by a sequence of data symbols \mathbf{s} , which is generated by mapping the binary data sequence \mathbf{u} onto data symbols. Below we present two different spatial coding techniques – Alamouti-type coding and repetition MIMO coding. For receiver-side combining strategies – selection diversity, equal-gain combining, and maximum-ratio combining – are investigated.

A. ALAMOUTI-TYPE CODING

The Alamouti scheme [28] is an orthogonal space-time block code that was originally invented for two transmit antennas. Its structure can be illustrated by the 2×2 transmission matrix

$$\mathbf{G} = \begin{bmatrix} s_k & s_{k+1} \\ -s_{k+1}^* & s_k^* \end{bmatrix}, \quad (9)$$

where s_k denotes the k th data symbol of \mathbf{s} . The rows of \mathbf{G} are related to the two consecutive transmission intervals $[kT_s, (k+1)T_s]$ and $[(k+1)T_s, (k+2)T_s]$, respectively. The

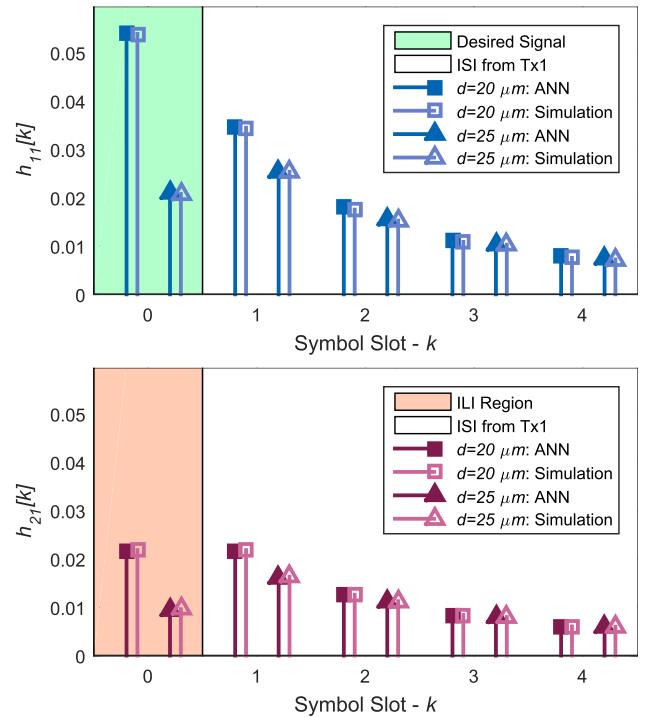


FIGURE 5. Comparison of channel coefficients from ANN and simulation data for different distances ($\alpha = 13 \mu\text{m}$, $r = 5 \mu\text{m}$, $D = 200 \mu\text{m}^2/\text{s}$, $T_s = 0.4 \text{ s}$).

columns of \mathbf{G} correspond to the two transmit antennas Tx_1 and Tx_2 , respectively. Accordingly, in the first time slot, $x_1[k] = s_k$ is transmitted via Tx_1 and $x_2[k] = s_{k+1}$ is transmitted simultaneously via Tx_2 . In the second time slot, $x_1[k+1] = -s_{k+1}^*$ is transmitted via Tx_1 and $x_2[k+1] = s_k^*$ is transmitted simultaneously via Tx_2 . As a result, the information of both data symbols is spread over both transmit antennas, which provides a spatial diversity gain in radio channels. Note that $\mathbf{G}^H \mathbf{G} = c \mathbf{I}$, where \mathbf{G}^H is the Hermitian of matrix \mathbf{G} , c is a constant factor, and \mathbf{I} denotes the identity matrix. Consequently, the Alamouti scheme is an orthogonal space-time block code for complex data symbols. With help of orthogonality, ILI can be canceled completely at the receiver side. Thus, the realization of a maximum-likelihood detector can be simplified, which makes the Alamouti scheme popular in radio-based communication systems without ISI.

In the case of ISI, however, orthogonality is not maintained any more. As a result, we must apply more complex detection algorithms such as maximum-likelihood sequence estimation (MLSE) [29]. Orthogonality can also be maintained by modifying the Alamouti transmission scheme, as shown in [30]. There is still a need, though, for equalization algorithms like MLSE. Furthermore, the modification introduces additional errors at the edges of the proposed transmission blocks.

The Alamouti scheme assumes complex data symbols that can either be positive or negative. In MC, however, the data symbols are typically represented by the amount of emitted molecules. Thus, the data symbols are non-negative

and real-valued. Consequently, (9) has to be modified to an Alamouti-type code [31] that avoids minus signs and complex conjugation. The focus of this work is on OOK. Accordingly, following the principle of (4), data bits are mapped onto data symbols $s_k \in \{0, N\}$ [17]–[19]. As suggested in [31], an adaptation to an Alamouti-type code can be done by the following two steps:

- 1) Since there are only real-valued integer values, the complex conjugate operation can be discarded.
- 2) The negative symbols can be replaced by the inverse symbol $\bar{s}_k := N - s_k$.

Applying those two steps to (9) leads to the transmission matrix of the Alamouti-type code:

$$\mathbf{G} = \begin{bmatrix} s_k & s_{k+1} \\ N - s_{k+1} & s_k \end{bmatrix}. \quad (10)$$

In [31], a maximum-likelihood detection metric was derived. It is shown that the Alamouti-type code has the same desirable properties as the conventional Alamouti scheme in terms of orthogonality. Note that in molecular communication, however, the system is affected by ISI and the orthogonality of the Alamouti-type code is no longer maintained. As well as for the conventional Alamouti scheme in channels with ISI, more complex detection algorithms like MLSE have to be applied for detection.

B. REPETITION MIMO CODING

Repetition MIMO coding [32] offers a simple intuitive alternative to orthogonal Alamouti scheme. In contrast to the Alamouti scheme, the information is coded only in the spatial domain, while the time domain is not exploited. In detail, exactly the same data symbol is transmitted via each transmit antenna at the same time. Accordingly for a 2×2 MIMO scenario, the transmission matrix is defined as

$$\mathbf{G} = \begin{bmatrix} s_k & s_k \end{bmatrix}. \quad (11)$$

Note that there is no orthogonality in the code and ILI cannot be canceled out at the receiver side. The ILI, however, will have a constructive influence of the signal strength. As a result, even in the presence of ISI, SISO detection algorithms can be used at the receiver side.

C. RECEIVER COMBINING

If there is more than one receive antenna, the received signals from each antenna have to be combined/selected, before detection can be performed. Normally, the selection/combining is done in one of three ways. With selection diversity (SD), the strongest signal of all antennas is selected for detection. In a molecular communication system in conjunction with OOK and ISI, it is hard to determine which antenna receives the strongest signal. For $u[k] = 0$ the signal with the minimum number of received molecules would be the strongest one, while for $u[k] = 1$ the signal with the maximum number of received molecules would be the strongest one. In this work, a symmetrical scenario is considered. Hence, the expected signal strength at both receive

antennas is equal. Therefore, without loss of generality, RX_1 is selected in the case of SD:

$$\begin{aligned} y_{SD}[k] &= y_1[k] \\ &= \sum_{\ell=0}^L h_{11}[\ell]x_1[k-\ell] + \sum_{\ell=0}^L h_{12}[\ell]x_2[k-\ell] + n_1[k]. \end{aligned} \quad (12)$$

Another combining strategy is equal-gain combining (EGC), where the signals of all receive antennas are equally weighted and combined. Adjusting the weighting factors to the corresponding channel quality leads to maximum-ratio combining (MRC), which is equal to a maximum-likelihood receiver. Consequently, channel knowledge is necessary at the receiver side. However, in the case of a symmetrical scenario, which leads to equal channels at both receive antennas, EGC is equal to MRC. As a result, EGC is considered in the following:

$$y_{EGC}[k] = y_1[k] + y_2[k]. \quad (13)$$

Due to the symmetrical system setting, the channel description for EGC can be further simplified. Considering that $h_{11}[\ell] = h_{22}[\ell]$ and $h_{12}[\ell] = h_{21}[\ell]$, (13) can be restated as

$$y_{EGC}[k] = \sum_{\ell=0}^L h[\ell] (x_1[k-\ell] + x_2[k-\ell]) + n[k], \quad (14)$$

where $h[\ell] \doteq h_{11}[\ell] + h_{12}[\ell]$ and $n[k] \doteq n_1[k] + n_2[k]$.

V. DETECTION ALGORITHMS

For the bit error analysis throughout this paper, we consider and adopt from [33] three different detection algorithms. First of all, the common fixed threshold detector (FTD)

$$\hat{u}[k] = \begin{cases} 1 & \text{if } y[k] > \eta \\ 0 & \text{if } y[k] \leq \eta \end{cases} \quad (15)$$

is used, where the threshold η is chosen to be optimal in terms of minimizing the BER. The optimal threshold is determined by means of an exhaustive search. Second, the low-complexity adaptive threshold detector (ATD) is applied:

$$\hat{u}[k] = \begin{cases} 1 & \text{if } y[k] > y[k-1] \\ 0 & \text{if } y[k] \leq y[k-1]. \end{cases} \quad (16)$$

Note that ATD does not need any channel knowledge and inherently benefits from ISI. The third algorithm is maximum-likelihood sequence estimation. It is applied with the suboptimal squared Euclidean distance branch metric

$$\gamma(y[k] | [\tilde{u}[k], \dots, \tilde{u}[k-L]]) = \left(y[k] - \sum_{\ell=0}^L N \hat{h}[\ell] \tilde{u}[k-\ell] \right)^2. \quad (17)$$

During the numerical analysis, it is assumed that $\hat{h}[\ell]$ are equal to the channel coefficients utilized in the equivalent discrete-time channel model. Depending on the considered

TABLE 1. Transmission example for Alamouti-type 2×2 MIMO scenario.

Discrete time step k	$k-2$	$k-1$	k	$k+1$
$x_1[k]$	s_{k-2}	$N - s_{k-1}$	s_k	$N - s_{k+1}$
$x_2[k]$	s_{k-1}	s_{k-2}	s_{k+1}	s_k

TABLE 2. Simulation parameters used for analysis. The default parameters are in bold face.

Parameter	Value
N	{500, 750, 1000 , 1250, 1500, 1750, 2000}
T_s [s]	{0.48, 0.6 , 0.8, 1.2}
$(L+1)T_s$ [s]	2.4
d [μm]	{10, 12.5, 15, 17.5, 20 , 22.5, 25}
a [μm]	{ 11 , 12, 13, 14, 15, 16, 17}
D [$\mu\text{m}^2/\text{s}$]	{50, 75, 100 , 125, 150, 175, 200}
r [μm]	5
K	10^6
R	1000

spatial coding and receiver combining strategy $\hat{h}[\ell]$ has to be adapted. For a SISO system, $\hat{h}[\ell]$ is set equal to the channel coefficients from (6). For repetition coding it yields $\hat{h}[\ell] = h[\ell]$ for SD and $\hat{h}[\ell] = 2h[\ell]$ for EGC, where $h[\ell]$ is defined as in (14).

In Alamouti-type coding, the information of two symbols is spread over two consecutive time slots. Thus, the branch metric can be evaluated jointly over both time slots. As a result, the branch metric has to be further adapted.

As an example, we present an Alamouti-type 2×2 MIMO transmission scenario for $L = 1$ in Table 1. It can be extended in the same way for arbitrary channel memory length L . For $L = 1$, we need to consider the transmission matrix \mathbf{G} in (10) including the corresponding ISI terms:

$$\mathbf{G}_1 = \begin{bmatrix} s_k & s_{k+1} & N - s_{k-1} & s_{k-2} \\ N - s_{k+1} & s_k & s_k & s_{k+1} \end{bmatrix}, \quad (18)$$

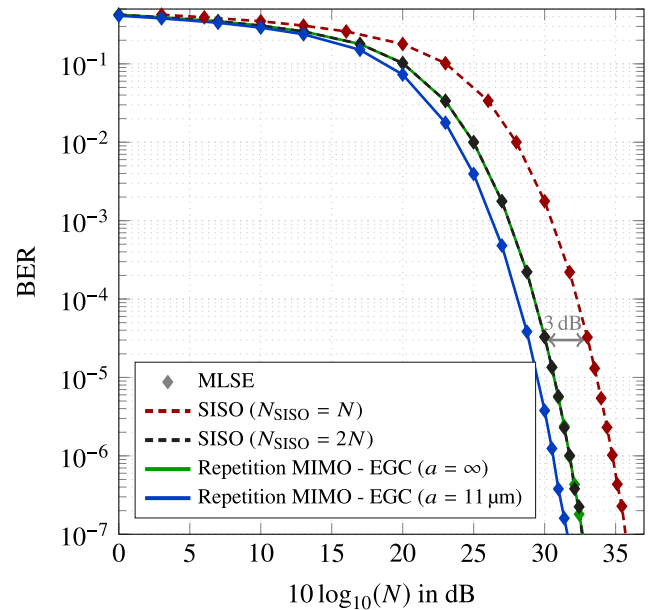
where \mathbf{G}_L represents the transmission matrix \mathbf{G} with L ISI terms. In our example, the last two columns correspond to the transmitted signal in the corresponding previous time slot by Tx₁ and Tx₂, respectively. Note that the first row's previous slot is $k-1$ and the second row's previous slot is k . In this case, the number of received molecules can be written as follows:

$$\begin{bmatrix} y_1[k] & y_2[k] \\ y_1[k+1] & y_2[k+1] \end{bmatrix} = \mathbf{G}_1 \begin{bmatrix} h_{11}[0] & h_{21}[0] \\ h_{12}[0] & h_{22}[0] \\ h_{11}[1] & h_{21}[1] \\ h_{12}[1] & h_{22}[1] \end{bmatrix} + [\mathbf{N}_1 \mathbf{N}_2], \quad (19)$$

where $\mathbf{N}_i = [n_i[k] \ n_i[k+1]]^T$. Assuming a symmetrical scenario and EGC, the branch metric can be adapted as shown in (20), as shown at the top of the next page.

VI. NUMERICAL RESULTS

In this section, results from the numerical analysis are presented. To analyze the effect of spatial coding and combining techniques, BER simulations are performed for SISO and 2×2 MIMO scenarios using the Poisson-binomial channel model

**FIGURE 6.** Bit error rate performance as a function of the number of molecules.

which is shown in (5). In detail, the impact of number of molecules N , symbol duration T_s , transmission distance d , separation distance a , and diffusion coefficient D on the BER is shown. The simulation parameters are summarized in Table 2, where K is the bit sequence length for one channel realization and R is the total number of channel realizations. Throughout the simulations, it is assumed that the remaining ISI is negligible after $(L+1)T_s = 2.4$ s. Accordingly, the channel memory length $L \in \{1, 2, 3, 4\}$ varies with different T_s . In the SISO scenarios, there is just a single transmit and a single receive antenna in the environment. Furthermore, we set the number of emitted molecules N to be twice as large as that in the MIMO scenarios. This guarantees a fair comparison between SISO and 2×2 MIMO scenarios by means of transmitting energy. Additionally in Section VI-G, the total receiver volume is normalized. To achieve this normalization the radius of each spherical receiver in 2×2 MIMO is $r_{\text{MIMO}} = r_{\text{SISO}} / \sqrt[3]{2} = r / \sqrt[3]{2}$.

A. SPATIAL DIVERSITY ANALYSIS

In classical wireless communication, spatial diversity is exploited to combat the effect of fading in transmission channels. The resulting diversity order Γ is commonly defined as the asymptotic slope of the BER curve plotted over the signal-to-noise ratio (SNR): $\text{BER} \propto (1/\text{SNR})^\Gamma$ for $\text{SNR} \rightarrow \infty$. Due to the amplitude dependent diffusion noise in DBMC, it is not as straightforward to define an SNR as it is in classical wireless communication. The amount of released molecules N , however, is proportional to the SNR [24]. To obtain logarithmic values which can be interpreted as SNR in dB, in Fig. 6 the BER is plotted over $10 \log_{10}(N)$.

Fig. 6 compares the SISO system (with and without power normalization) to the repetition MIMO system with EGC,

$$\begin{aligned} \gamma(y[k], y[k+1]|\tilde{u}[k+1], \tilde{u}[k], \tilde{u}[k-1], \tilde{u}[k-2]) = & \left[y[k] - Nh[0](\tilde{u}[k] + \tilde{u}[k+1]) - Nh[1](\tilde{u}[k-2] - \tilde{u}[k-1] + 1) \right]^2 \\ & + \left[y[k+1] - Nh[0](\tilde{u}[k] - \tilde{u}[k+1] + 1) - Nh[1](\tilde{u}[k] + \tilde{u}[k+1]) \right]^2 \end{aligned} \quad (20)$$

both in conjunction with the MLSE detector. The focus here is on repetition MIMO with EGC only, since it outperforms the other techniques under investigation as shown in Sec. VI-B to Sec. VI-G. When power normalization is not applied, there is the typical gain of about 3 dB (a factor of two in linear scale) between the SISO system and the 2×2 MIMO system with separation distance $a = \infty$. This gain is due to an array gain, which occurs when multiple transmit/receive antennas are used. The transmit power and receive area is doubled, which is equivalent to the use of two transmit and receiving antennas in radio-based wireless transmissions. It will disappear when power normalization is applied to the SISO scenario as shown in Fig. 6. At separation distance $a = 11 \mu\text{m}$, the array gain is even larger than 3 dB. The additional gain comes from the increasing total energy of the channel coefficients. If $a = \infty$, there is no ILI and the channel energy of each direct link is equal to the channel energy of the SISO link. If $a = 11 \mu\text{m}$, however, the channel energy of the direct links are decreasing (due to the second absorbing sphere) while the ILI channels are increasing. The total channel energy of all links will be larger than in the $a = \infty$ case.

From Fig. 6 it can be observed that the asymptotic slope of the BER curve (i. e., the diversity order) is not changing when it comes to MIMO systems. Consequently, there is no fading or fading-like effect in the standard DBMC channel, at least not for the system under investigation. Fading might occur in scenarios, where an obstacle is placed between the transmitter and the receiver. A detailed analysis of different scenarios, however, is left for future work. Conclusively, all the performance gains that are achieved by applying spatial diversity algorithms throughout this work are due to an array gain and not due to a spatial diversity gain.

B. EFFECT OF NUMBER OF EMITTED MOLECULES

In Fig. 7a, the effect of the number of emitted molecules on the BER is shown. If N is increased, more molecules reach the receiving spheres. Furthermore, the amplitude dependent diffusion noise is relatively getting less. Consequently, N is proportional to the signal strength. As a result, all detection algorithms perform better, when N is increased. The simple FTD suffers from the strong ISI in the system and is not able to detect in a reasonable manner with its fixed threshold. The ATD, in contrast, benefits from the ISI in the system [33]. Consequently, ATD outperforms FTD in terms of BER. The best BER performance is achieved by MLSE, because it implies channel equalization, which counteracts ISI. In the case of FTD, the investigated spatial algorithms do

not bring any enhancement compared to the SISO case for the parameters under investigation. In contrast, repetition MIMO with EGC for ATD slightly outperforms SISO transmission in a region with few molecules. If the power normalization of the SISO case (the emitted number of molecules in the SISO case is twice as large as in the 2×2 MIMO case) is neglected, even repetition MIMO in conjunction with SD achieves a BER slightly below SISO performance. However, the array gain for ATD is not significant. For MLSE, the array gain can be more clearly observed. The maximum BER improvement of repetition MIMO with EGC over the SISO case is by a factor of almost 10, yet repetition MIMO with SD shows a degradation by a factor of approximately 10 to 10^2 . However, neglecting the power normalization leads to a maximum improvement of almost 400 for EGC and of approximately 10 for SD. Interestingly, for the system under investigation, Alamouti-type coding does not show any array gain. This can be explained by the ILI in the system. Note that ILI in repetition MIMO constructively contribute to the signal strength. For Alamouti-type coding, however, the ILI acts competitive and thus more destructive. The Alamouti code does not perform well for channels with unipolar properties as shown in [34] for the free-space optical channel. The main degrading factor in the molecular channel, however, comes from the ISI and the resulting ILI.

C. EFFECT OF SYMBOL DURATION

Fig. 7b depicts the effect of symbol duration on the BER performance. In general, an increasing symbol duration is beneficial for the communication system, because the molecules have more time to hit the Rx during their desired symbol duration and Rx accumulates over a longer time interval. As a result, the effect of ISI lessens and detection performance increases. The only exception is ATD, which inherently benefits from ISI. Therefore, in the scenario under investigation, ATD is superior to FTD for $T_s \leq 0.8 \text{ s}$. For $T_s > 0.8 \text{ s}$, the BER of ATD increases slightly, whereas the BER of FTD improves remarkably. As expected, the best detection performance is achieved by MLSE. While there is no significant array gain in conjunction with ATD, repetition MIMO in conjunction with EGC and FTD outperforms the SISO case by a factor of almost 10 at $T_s = 1.2 \text{ s}$. As shown in Section VI-B, for MLSE the size of the gap between repetition MIMO with EGC and that of a SISO system is larger by a factor of almost 10. Furthermore, MLSE repetition MIMO with SD does not show an array gain, at least not for the assumed power normalization. As already discussed in Section VI-B,

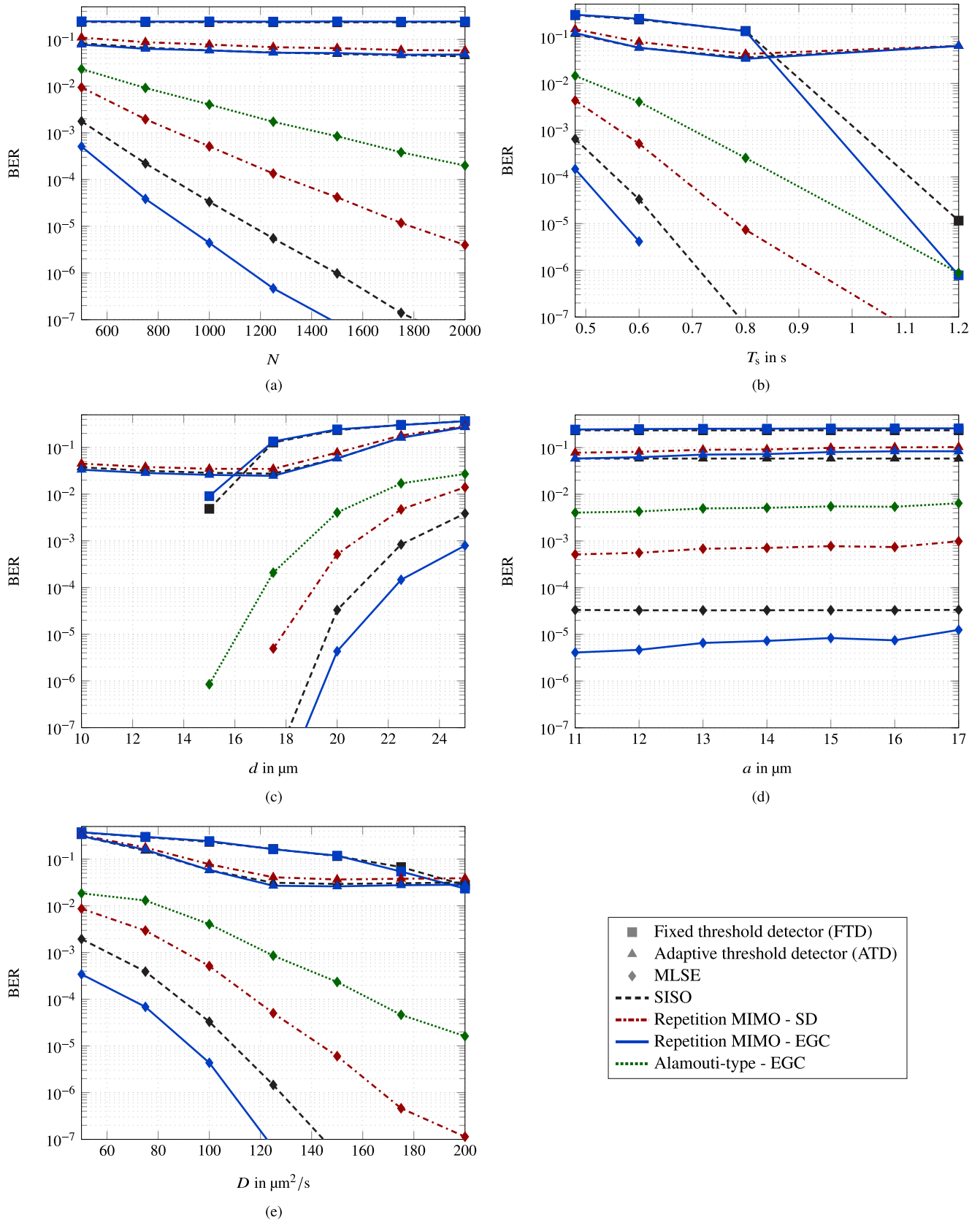


FIGURE 7. Bit error rate performance as a function of the number of molecules (a), symbol duration (b), transmitting distance (c), separation distance (d), and diffusion coefficient (e). If the corresponding parameter is not varying, it is fixed to $N = 1000$, $T_s = 0.6$ s, $d = 20$ μm , $a = 11$ μm , and $D = 100$ $\mu\text{m}^2/\text{s}$.

Alamouti-type coding with EGC offers no improvement over the SISO scenario.

D. EFFECT OF TRANSMISSION DISTANCE

In Fig. 7c, the effect of the transmission distance on the system performance is shown. In general, shorter transmission distances provide that more molecules are absorbed by Rx, which increases the signal strength. If the symbol duration is fixed, it also reduces the effect of ISI inside the system. If transmission distance decreases, the BER of all detection algorithms decreases (with the exception of ATD, which inherently benefits from ISI). For long distances ($17.5 \mu\text{m} \leq d \leq 25 \mu\text{m}$), ATD detection performance is superior to FTD, but for short distances ($d < 17.5 \mu\text{m}$), FTD is superior to ATD. As expected, MLSE achieves the best BER performance for all distances under consideration. As in Section VI-B and Section VI-C, there is no significant array gain regarding ATD for the scenario under investigation. Furthermore, the array gain of repetition MIMO with EGC and MLSE is by a factor of almost 10, while Alamouti-type coding offers no gain at all. In contrast to Fig. 7b, there is also no array gain observed for FTD.

E. EFFECT OF ANTENNA SEPARATION

In Fig. 7d, the effect of the antenna separation on the MIMO system performance is shown. All MIMO schemes show a similar trend. If the antenna separation is increased, the BER is decreased. The reason for that is in the spatial gain from the ILI, because increasing a will lead to a decreasing ILI. Note that even for $a = 17 \mu\text{m}$ there is an array gain of repetition MIMO with EGC and MLSE.

F. EFFECT OF DIFFUSION COEFFICIENT

In Fig. 7c, the effect of the diffusion coefficient on the system performance is shown. In general, D describes the mobility of a particle inside a medium. Accordingly, D has an impact on the channel impulse response. In fact, a larger diffusion coefficient leads to a more spiky channel impulse response, whereas a lower diffusion coefficient leads to a more flat channel impulse response. As a result, the ISI is decreased when D is increased. Consequently, all investigated detection algorithms perform better for larger D . While the array gain from repetition MIMO with EGC for ATD increases with D , it decreases with FTD. For the scenario under investigation, the difference between SISO MLSE and repetition MIMO with EGC and MLSE is constant by a factor of approximately 10. As can be seen in Fig. 7a-7d, there is no array gain obtained by Alamouti-type coding.

G. RECEIVER VOLUME NORMALIZATION

For a fair comparison between SISO and MIMO systems, the effective receiver volume can be normalized as well. Without volume normalization, i. e. $r_{\text{MIMO}} = r_{\text{SISO}} = r$, the effective receiver volume in the MIMO scenario is larger by a factor proportional to the number of receivers. To normalize the effective receiver volume in the 2×2 MIMO scenario under

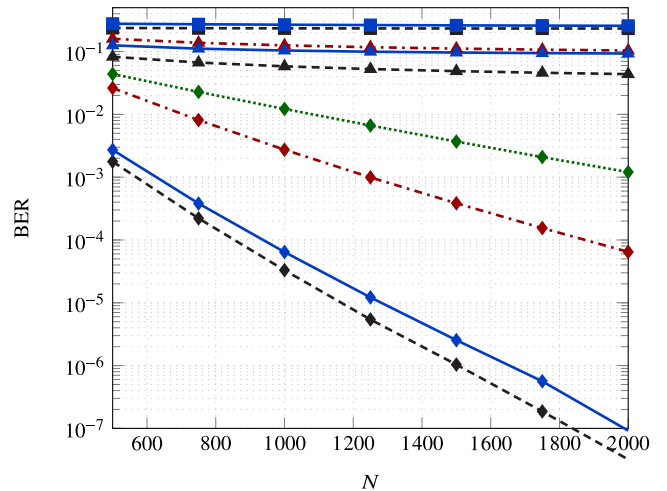


FIGURE 8. Bit error rate performance as a function of the number of molecules ($T_s = 0.6 \text{ s}$, $d = 20 \mu\text{m}$, $\sigma = 11 \mu\text{m}$, and $D = 100 \mu\text{m}^2/\text{m}$). The spherical receiver radius is normalized to $r_{\text{MIMO}} = r_{\text{SISO}}/\sqrt[3]{2} = r/\sqrt[3]{2}$. The legend is given in Fig. 7.

investigation, the radii of the MIMO receivers are normalized as $r_{\text{MIMO}} = r_{\text{SISO}}/\sqrt[3]{2} = r/\sqrt[3]{2}$. Fig. 8 shows the resulting BER curves when the number of released molecules is changed. Compared to Fig. 7a, all MIMO systems perform worse than without volume normalization. Even for repetition MIMO with EGC and MLSE detection, there is no longer an array gain visible in the results. Only without power normalization, repetition MIMO with EGC and MLSE achieve an array gain. The effect of volume normalization to the simulation results of varying symbol duration, transmission distance, separation distance, and diffusion coefficient will behave similar. Thus, those results are not presented in detail.

VII. CONCLUSION

In this paper, we have presented a diffusion-based molecular 2×2 MIMO communication system in a 3-D environment. Channel coefficients were obtained from a trained ANN and incorporated into performance evaluations. Motivated from the potential of spatial diversity in classical wireless communication, this paper introduced different spatial coding and combining techniques to the area of MC and analyzed their performances. At the transmitter side, Alamouti-type coding and repetition MIMO coding were proposed. At the receiver side, selection diversity, equal-gain combining, and maximum-ratio combining were presented as receiver combining strategies. In addition, fixed threshold detection, adaptive threshold detection and maximum-likelihood sequence estimation were adapted to the 2×2 MIMO scenario.

It was shown that there is no fading-like process in the molecular channel under investigation. Consequently, there is no diversity gain exploited in the system but an array gain. The array gain was studied by means of BER simulations, where different system parameters were varied to show the effect on the system performance. Similar to the SISO case,

MLSE outperforms FTD and ATD, while ATD outperforms FTD when more ISI is present, since ATD profits from ISI. Furthermore, FTD and MLSE performance benefit from a higher number of emitted molecules, a larger symbol duration, a shorter transmission distance and a higher diffusion coefficient. A significant array gain can only be achieved by repetition MIMO with EGC and MLSE for the scenario under investigation. In contrast, Alamouti-type coding fails to show a practical performance in the context of MC. Even in conjunction with MLSE, it suffers from the discrepancy between averaged and actual channel coefficients. The array gain depends on the antennas separation distance. The simulation showed that the best BER performance is achieved, when the receive and transmit antennas are as close together as possible. From energy perspective, it might also be reasonable to normalize the receiver volumes. In conjunction with power normalization, there is no array gain observed for the system under investigation. Without power normalization, repetition MIMO with EGC and MLSE will still be able to achieve an array gain. In future practical realizations, however, there might be standard nanomachines with a fixed size available. In those cases, multiple receivers could be used for achieving an array gain. In addition, it might be more practical to use several smaller NMs instead of a single larger NM to navigate through the human body. Compared to a SISO system, the additional complexity of a repetition MIMO EGC system is negligibly small. At the transmitter side, the same sequence has to be transmitted by each nanomachine. This could be realized, for example, by controlling the release of molecules from other nanomachine through the release of molecules from a reference nanomachine. At the receiver side, EGC is a simple summation of the received signal, which is a common thing in biological systems. Since the modeling and analysis of energy costs is an independent work, a more detailed study is left for future work. In conclusion, there is no spatial diversity gain but an array gain achievable for the DBMC channel under investigation. If possible, repetition MIMO with maximum-ratio combining and MLSE should be performed. Depending on the normalization point of view, the array gain can disappear completely.

Future work will include the realization of MIMO algorithms in practical systems, modeling the energy costs, the comparison of system complexities, analyzing spatial diversity for unsymmetrical cases and scenarios with obstacles between transmitter and receiver, and expanding the system to a higher number of transmit and/or receive antennas.

REFERENCES

- [1] N. Farsad, H. B. Yilmaz, A. Eckford, C.-B. Chae, and W. Guo, "A comprehensive survey of recent advancements in molecular communication," *IEEE Commun. Surveys Tuts.*, vol. 18, no. 3, pp. 1887–1919, 3rd Quart., 2016.
- [2] I. F. Akyildiz, F. Brunetti, and C. Blázquez, "Nanonetworks: A new communication paradigm," *Comput. Netw.*, vol. 52, no. 12, pp. 2260–2279, 2008.
- [3] B. Atakan, O. B. Akan, and S. Balasubramaniam, "Body area nanonetworks with molecular communications in nanomedicine," *IEEE Commun. Mag.*, vol. 50, no. 1, pp. 28–34, Jan. 2012.
- [4] Y. Xia et al., "One-dimensional nanostructures: Synthesis, characterization, and applications," *Adv. Mater.*, vol. 15, no. 5, pp. 353–389, 2003.
- [5] T. Nakano, M. Moore, A. Enomoto, and T. Suda, "Molecular communication technology as a biological ICT," in *Biological Functions for Information and Communication Technologies*. Berlin, Germany: Springer, 2011, pp. 49–86.
- [6] T. Nakano, A. W. Eckford, and T. Haraguchi, *Molecular Communication*. Cambridge, U.K.: Cambridge Univ. Press, 2013.
- [7] W. Guo et al., "Molecular communications: Channel model and physical layer techniques," *IEEE Wireless Commun.*, vol. 23, no. 4, pp. 120–127, Aug. 2016.
- [8] M. Pierobon and I. F. Akyildiz, "A physical end-to-end model for molecular communication in nanonetworks," *IEEE J. Sel. Areas Commun.*, vol. 28, no. 4, pp. 602–611, May 2010.
- [9] A. Noel, K. C. Cheung, and R. Schober, "Optimal receiver design for diffusive molecular communication with flow and additive noise," *IEEE Trans. NanoBiosci.*, vol. 13, no. 3, pp. 350–362, Sep. 2014.
- [10] L.-S. Meng, P.-C. Yeh, K.-C. Chen, and I. F. Akyildiz, "MIMO communications based on molecular diffusion," in *Proc. IEEE Glob. Commun. Conf. (GLOBECOM)*, Dec. 2012, pp. 5380–5385.
- [11] B.-H. Koo, C. Lee, H. B. Yilmaz, N. Farsad, A. Eckford, and C.-B. Chae, "Molecular MIMO: From theory to prototype," *IEEE J. Sel. Areas Commun.*, vol. 34, no. 3, pp. 600–614, Mar. 2016.
- [12] Y. Lu, M. D. Higgins, A. Noel, M. S. Leeson, and Y. Chen, "The effect of two receivers on broadcast molecular communication systems," *IEEE Trans. NanoBiosci.*, vol. 15, no. 8, pp. 891–900, Dec. 2016.
- [13] Y. Murin, M. Chowdhury, N. Farsad, and A. Goldsmith, "Diversity gain of one-shot communication over molecular timing channels," in *Proc. IEEE Global Commun. Conf. (GLOBECOM)*, Dec. 2017, pp. 1–6.
- [14] C. Lee et al., "Molecular MIMO communication link," in *Proc. IEEE Int. Conf. Comput. Commun. (INFOCOM)*, 2015, pp. 13–14.
- [15] K. V. Srinivas, A. W. Eckford, and R. S. Adve, "Molecular communication in fluid media: The additive inverse Gaussian noise channel," *IEEE Trans. Inf. Theory*, vol. 58, no. 7, pp. 4678–4692, Jul. 2012.
- [16] H. B. Yilmaz, A. C. Heren, T. Tugcu, and C.-B. Chae, "Three-dimensional channel characteristics for molecular communications with an absorbing receiver," *IEEE Commun. Lett.*, vol. 18, no. 6, pp. 929–932, Jun. 2014.
- [17] M. S. Kuran, H. B. Yilmaz, T. Tugcu, and I. F. Akyildiz, "Modulation techniques for communication via diffusion in nanonetworks," in *Proc. IEEE Int. Conf. Commun. (ICC)*, Jun. 2011, pp. 1–5.
- [18] H. B. Yilmaz and C.-B. Chae, "Simulation study of molecular communication systems with an absorbing receiver: Modulation and ISI mitigation techniques," *Simul. Model. Pract. Theory*, vol. 49, pp. 136–150, Dec. 2014.
- [19] N.-R. Kim and C.-B. Chae, "Novel modulation techniques using isomers as messenger molecules for nano communication networks via diffusion," *IEEE J. Sel. Areas Commun.*, vol. 31, no. 12, pp. 847–856, Dec. 2013.
- [20] M. J. Moore and T. Nakano, "Oscillation and synchronization of molecular machines by the diffusion of inhibitory molecules," *IEEE Trans. Nanotechnol.*, vol. 12, no. 4, pp. 601–608, Jul. 2013.
- [21] M. U. Mahfuz, D. Makrakis, and H. Mouftah, "Spatiotemporal distribution and modulation schemes for concentration-encoded medium-to-long range molecular communication," in *Proc. IEEE Biennial Symp. Commun. (QBSC)*, May 2010, pp. 100–105.
- [22] M. U. Mahfuz, D. Makrakis, and H. T. Mouftah, "On the characterization of binary concentration-encoded molecular communication in nanonetworks," *Nano Commun. Netw.*, vol. 1, no. 4, pp. 289–300, Dec. 2010.
- [23] I. Llatser, A. Cabellos-Aparicio, M. Pierobon, and E. Alarcón, "Detection techniques for diffusion-based molecular communication," *IEEE J. Sel. Areas Commun.*, vol. 31, no. 12, pp. 726–734, Dec. 2013.
- [24] M. Damrath, S. Korte, and P. A. Hoeher, "Equivalent discrete-time channel modeling for molecular communication with emphasize on an absorbing receiver," *IEEE Trans. NanoBiosci.*, vol. 16, no. 1, pp. 60–68, Jan. 2017.
- [25] G. Genc, Y. E. Kara, H. B. Yilmaz, and T. Tugcu, "ISI-aware modeling and achievable rate analysis of the diffusion channel," *IEEE Commun. Lett.*, vol. 20, no. 9, pp. 1729–1732, Sep. 2016.
- [26] H. B. Yilmaz and C.-B. Chae, "Arrival modelling for molecular communication via diffusion," *Electron. Lett.*, vol. 50, no. 23, pp. 1667–1669, 2014.
- [27] C. Lee, H. B. Yilmaz, C.-B. Chae, N. Farsad, and A. Goldsmith, "Machine learning based channel modeling for molecular MIMO communications," in *Proc. IEEE Int. Workshop Sig. Proc. Adv. Wireless Commun. (SPAWC)*, Apr. 2017, pp. 1–6.
- [28] S. Alamouti, "A simple transmit diversity technique for wireless communications," *IEEE J. Sel. Areas Commun.*, vol. 16, no. 8, pp. 1451–1458, Oct. 1998.

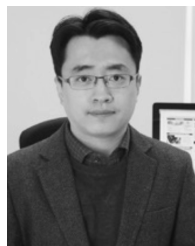
- [29] J. Mietzner and P. A. Hoeher, "Boosting the performance of wireless communication systems: Theory and practice of multiple-antenna techniques," *IEEE Commun. Mag.*, vol. 42, no. 10, pp. 40–47, Oct. 2004.
- [30] E. Lindskog and A. Paulraj, "A transmit diversity scheme for channels with intersymbol interference," in *Proc. IEEE Int. Conf. Commun. (ICC)*, Jun. 2000, pp. 307–311.
- [31] M. K. Simon and V. A. Vilnrotter, "Alamouti-type space-time coding for free-space optical communication with direct detection," *IEEE Trans. Wireless Commun.*, vol. 4, no. 1, pp. 35–39, Jan. 2005.
- [32] S. G. Wilson, M. Brandt-Pearce, Q. Cao, and M. Baedke, "Optical repetition MIMO transmission with multipulse PPM," *IEEE J. Sel. Areas Commun.*, vol. 23, no. 9, pp. 1901–1910, Sep. 2005.
- [33] M. Damrath and P. A. Hoeher, "Low-complexity adaptive threshold detection for molecular communication," *IEEE Trans. NanoBiosci.*, vol. 15, no. 3, pp. 200–208, Apr. 2016.
- [34] M. Safari and M. Uysal, "Do we really need OSTBCs for free-space optical communication with direct detection?" *IEEE Trans. Wireless Commun.*, vol. 7, no. 11, pp. 4445–4448, Nov. 2008.



MARTIN DAMRATH (S'16) received the M.Sc. degree in electrical engineering from the University of Kiel, Germany, in 2014, where he is currently pursuing the Dr.Ing. (Ph.D.) degree with the Faculty of Engineering. Since 2014, he has been a Research and Teaching Assistant with the Information and Coding Theory Laboratory, University of Kiel, for his Ph.D. study. His current research interests include high-order modulation schemes, superposition modulation, and diffusion-based molecular communication.



H. BIRKAN YILMAZ (S'10–M'12) received the B.S. degree in mathematics in 2002, and the M.Sc. and Ph.D. degrees in computer engineering from Boğaziçi University in 2006 and 2012, respectively. He was with the Yonsei Institute of Convergence Technology, Yonsei University, South Korea. He is currently a Post-Doctoral Researcher with the Department of Network Engineering, Polytechnic University of Catalonia, Spain. His research interests include cognitive radio, spectrum sensing, molecular communications, and detection and estimation theory. He is a member of the Turkish Mathematical Society. He received the TUBITAK National Ph.D. Scholarship during his Ph.D. studies. He was a co-recipient of the Best Paper Award from AICT (2010) and ISCC (2012) and the Best Demo Award from IEEE INFOCOM (2015).



CHAN-BYOUNG CHAE (SM'12) received the Ph.D. degree in electrical and computer engineering from The University of Texas at Austin in 2008. He was a member of the Wireless Networking and Communications Group with The University of Texas at Austin. He was a Research Engineer with the Telecommunications R&D Center, Samsung Electronics, Suwon, South Korea, from 2001 to 2005. He was with Harvard University, Cambridge, MA, USA, from 2008 to 2009, as a Post-Doctoral Research Fellow. He was with Bell Labs, Murray Hill, NY, USA, from 2009 to 2011, as a Member of Technical Staff. He is currently the Underwood Distinguished Professor with the School of Integrated Technology, Yonsei University. He has served/serves as an Editor for the IEEE TRANSACTIONS ON WIRELESS COMMUNICATIONS (since 2012), the IEEE/KICS JOURNAL OF COMMUNICATIONS NETWORKS (since 2012), the IEEE TRANSACTIONS ON MOLECULAR, BIOLOGICAL, AND MULTI-SCALE COMMUNICATIONS (since 2015), the IEEE WIRELESS COMMUNICATIONS LETTERS (since 2016), and the *IEEE Communications Magazine* (since 2016).

He was a recipient/co-recipient of the KSEA-KUSCO Scholarship (2007), the IEEE VTS Daniel E. Noble Fellowship Award (2008), the two Gold Prizes (first) from the 14th/19th Humantech Paper Contests, the IEEE Com-Soc AP Outstanding Young Researcher Award (2012), the KICS Haedong Young Scholar Award (2013), the *IEEE Signal Processing Magazine* Best Paper Award (2013), the IEIE/IEEE Joint Award for Young IT Engineer of the Year (2014), the Best Young Professor Award from the College of Engineering, Yonsei University (2015), the IEEE INFOCOM Best Demo Award (2015), the Underwood Distinguished Professor Award (2016), the Yonam Research Award from the LG Yonam Foundation (2016), the Outstanding Professor Award from IITP (2016), the Award of Excellence in Leadership of 100 Leading Core Technologies for Korea 2025 from the National Academy of Engineering of Korea (2017), the Outstanding Teaching Award from Yonsei University (2017), the IEEE/KICS JOURNAL OF COMMUNICATIONS AND NETWORKS Best Paper Award (2018), and the Outstanding Achievement Award (Highly Cited Researcher) from Yonsei University (2018). He also received the Korea Government Fellowship during his Ph.D. studies.



PETER ADAM HOEHER (F'14) received the Dipl.Ing. (M.Sc.) degree in electrical engineering from RWTH Aachen University, Aachen, Germany, in 1986, and the Dr.Ing. (Ph.D.) degree in electrical engineering from the University of Kaiserslautern, Kaiserslautern, Germany, in 1990. From 1986 to 1998, he was with the German Aerospace Center, Oberpfaffenhofen, Germany. From 1991 to 1992, he was on leave at AT&T Bell Laboratories, Murray Hill, NJ, USA. In 1998, he joined the University of Kiel, Germany, where he is currently a Full Professor of electrical and information engineering. His research interests are in the general area of communication theory and applied information theory with applications in wireless radio communications, optical wireless communications, molecular communications, underwater communications, and simultaneous wireless information and power transfer. Since 2014, he has been an IEEE Fellow for the contributions to decoding and detection that include reliability information. He received the Hugo-Denkmeier-Award in 1990 and the ITG Award 2007. From 1999 to 2006, he has served as an Associated Editor for the IEEE TRANSACTIONS ON COMMUNICATIONS.

• • •